表9 DLB の臨床診断基準

| | |
|---|---|
1. 必須症状
- 社会的・職業的機能に障害を及ぼす程度の進行性の認知機能障害が存在すること. 初期には顕著な記憶障害が目立たないこともあるが, 進行とともに明らかになる. 注意, 遂行機能, 視空間機能の障害がとくに目立つこともある.

2. 中核症状 (probable DLB には二つが, possible DLB には一つが必要)
- 注意や覚醒レベルの著明な変化を伴う認知機能の変動
- 繰り返し現れる詳細で具体的な内容の幻視
- 特発性のパーキンソニズム

3. 示唆症状 (一つ以上の中核症状に一つ以上の示唆症状が加われば probable DLB と診断される. 中核症状はまったくないが一つ以上の示唆症状があれば possible DLB と診断できる)
- REM 睡眠行動異常
- 抗精神病薬への過敏性の亢進
- SPECT や PET で認められる基底核へのドパミンの取り込み低下

4. 支持症状
- 繰り返す転倒や失神
- 一過性の原因がはっきりしない意識障害
- 重度の自律神経障害 (例:起立性低血圧, 排尿障害)
- 幻視以外の幻覚
- 系統的な妄想
- 抑うつ
- CT/MRI での側頭葉内側部の構造が比較的保たれていること
- SPECT/PET で明らかになる後頭葉を含む全般的な血流/代謝の低下
- MIBG 心筋シンチグラフィー取り込みの低下
- 脳波上, 側頭葉の一過性鋭波を伴う著明な徐波活動

態は不明であるが, その構成成分が α シヌクレインであることがわかってきた.

もっとも新しい診断基準 (McKeith *et al.*, 2005) (表9) では臨床症状と神経画像所見とから, possible DLB または probable DLB の2段階に診断するようになっている. 臨床的には probable DLB の診断基準を満たした場合に DLB と診断する. 特徴的な臨床症状は診断基準の中核症状に取り上げられている三徴, すなわち認知機能の変動, 幻視, 特発性パーキンソニズムである. 幻視は他の認知症では頻度が少ない症状であるため鑑別にとくに重要である. 人や小動物がみえるということが多く, せん妄のないときでも認められる. 診断基準には含まれていないが, 誤認妄想が認められるのも特徴である. 病初期から自分の家を自分の家でないといったり, 家人を家人でないとか偽物であるといったりする. 発症, 進行は緩徐で, AD と同様に記憶障害も認められるが AD と比較すると記憶障害, とくに再生の障害が軽い. 一方, DLB では AD よりも視覚認知障害が強い. たとえば, いくつかの物品の線画が重ねて描かれた錯綜図からそれぞれの線画を弁別することができなくなる. また図形の模写が苦手になる. そしてこの視覚認知障害が DLB の幻視や一部の誤認妄想の発現に関与している可能性がある.

magnetic resonance imaging (MRI) では, びまん性の脳萎縮が認められる. AD と比較すると海馬領域の萎縮は軽度で, 側脳室下角の拡大も軽度である. positron emission tomography (PET) や single photon emission computed tomography (SPECT) は診断に有用で, 後頭葉領域の機能低下が特徴的な所見である (図6). 最近, 鑑別診断に metaiodobenzylguanidine (MIBG) 心筋シンチグラフィーも利用されている. DLB では MIBG の取り込みが著しく低下する.
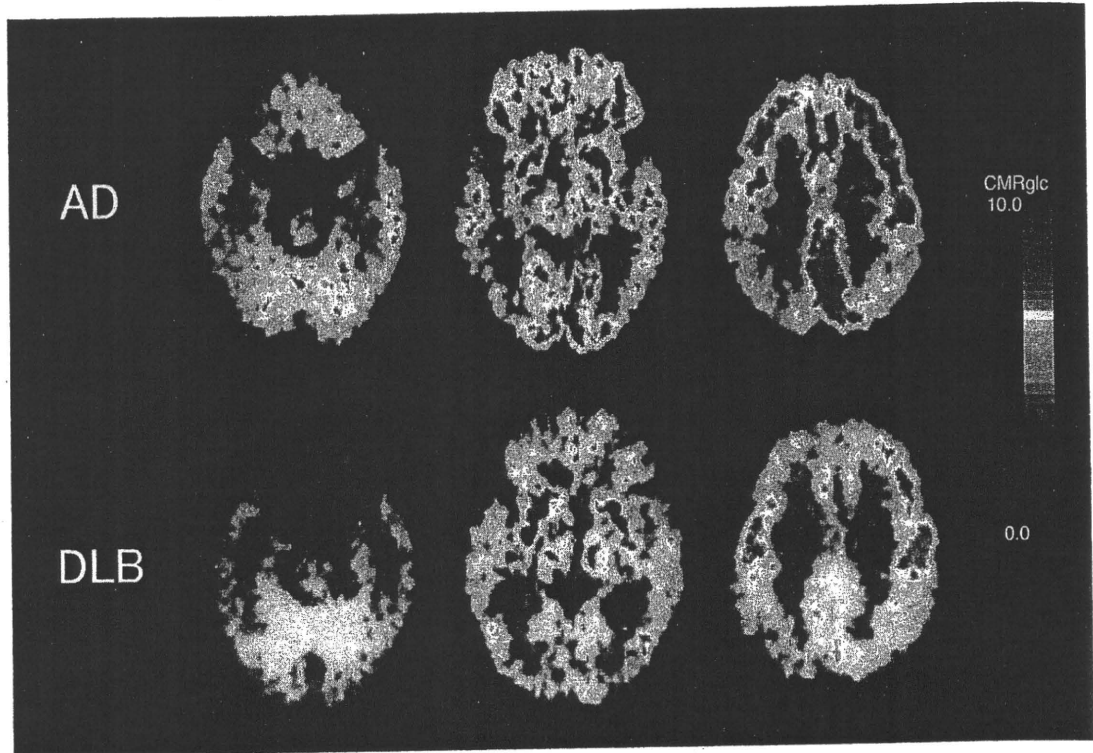
図6　DLB 患者と AD 患者との FDG-PET 画像の比較
上の段の AD の画像と比べると DLB では後頭葉の糖代謝低下が著しい.

　治療薬としては，保険適用はないが，コリンエステラーゼ阻害薬が有効である．DLB では幻視や認知機能の変動が著しく改善することがあり，AD よりもよく効くとの印象をもつ臨床家は多い．DLB ではマイネルト基底核の神経細胞の脱落が AD よりも顕著でアセチルコリン系の障害が強いためと考えられている．DLB では精神行動障害が顕著であるため抗精神病薬を使用せざるをえないことがある．しかし示唆症状に明記されているように抗精神病薬に対する過敏性を有する．このため，少量の抗精神病薬の投与によって起立性低血圧などが生じ，転倒，骨折が起こることもある．したがって，やむを得ない場合に限り，副作用の少ない非定型抗精神病薬を細心の注意を払いながら投与する態度が必要である．

### 10.7.2　前頭側頭葉変性症 （frontotemporal lobar degeneration : FTLD）

　前頭葉か側頭葉に限局性の脳萎縮を認め，人格変化，脱抑制，常同症などの独特の精神行動障害を呈し社会的接触性が障害されるが，一方，記憶障害，見当識障害，視空間認知障害などの認知障害は比較的軽度の疾患である．以前はピック病と呼ばれていたが，ピック病の特徴的な病理学的所見とされていたピック嗜銀球を認めない患者が存在することがしられるようになり，ピック嗜銀球を認めない病態もピック病に含むか否かなど議論となった．その後，臨床診断基準の必要性も高まり，何度かの改訂を経て，現在，FTLD という概念で臨床診断基準が提案されている （Neary *et al.,* 1998）．この臨床診断基準では FTLD を前頭側頭型認知症，進行性非流暢性失語，意味認知症に三分類している．

　a.　前頭側頭型認知症 （frontotemporal dementia : FTD）
　FTLD の中核的な病型で，表 10 の臨床的診断特徴に示されているように，さまざまな前頭葉性の

表10 FTD の臨床的診断特徴

1. 中核的特徴（すべて必要）
   ・潜行性に発症し徐々に進行する
   ・早期からの社会的対人関係の低下
   ・早期からの対人接触の調整障害
   ・早期からの情動の鈍麻
   ・早期からの病識の低下

2. 支持する診断的特徴
   A. 行動異常
   ・衛生・整容の障害
   ・思考の硬直化・柔軟性の消失
   ・易転導性と維持困難
   ・口唇傾向・食行動変化
   ・保続的・常同的行動
   ・利用行動
   B. 発話と言語
   ・発話量の変化
     (a) 自発性の低下と発話の簡略化
     (b) 発話の亢進
   ・常同的発話
   ・反響言語
   ・保続
   ・緘黙
   C. 身体所見
   ・原始反射
   ・失禁
   ・無動・固縮・振戦
   ・低く不安定な血圧
   D. 検査所見
   ・神経心理学的検査：重度の健忘・失語・空間認知障害は伴わないが前頭葉テストでは障害が明らかになる
   ・脳波検査：正常
   ・脳画像検査（形態／機能画像）：著明な前頭葉，または側頭葉前方部の異常

行動障害が認められる．非常に自己中心的になり，したいことはせずにはおられなくなる．逆にしたくないことはまったくしない．たとえば，店先に並んでいるお饅頭を食べたくなると制止することができず，お金を払わずに食べてしまうことがある．この行動は脱抑制と表現される．また診察中，診療者の質問に対しても十分に考えずに「知らん」，「わからん」と単純に答えることがあり，この様子は考え無精と呼ばれる．また診察途中でも帰りたくなると帰ろうとし，これは立ち去り行動と表現される．その他，単純な行為であれば膝をさする，複雑な物であれば雨戸を閉め続ける，同じ物を食べ続けるなど同じ動作をし続ける常同行動，同じことをいい続ける滞続言語も認められる．また非影響性の亢進も目立つ症状で，目に入る字を読まずにはおられなかったり，いくら制止しても診療者の真似をせずにはおられなかったり（模倣行動），目の前の物品を使わずにはおれなかったりする（利用行動）こともある．その一方で，意欲低下，発動性の低下も認める．MRI では限局性の強い前頭葉の萎縮を認めるか（図7），MRI で萎縮が明らかでなくても SPECT や PET では前頭葉を中心とした限局性の機能低下を認める．
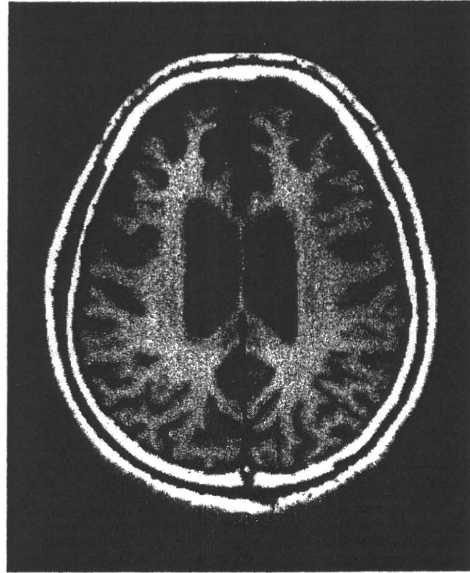
図7　FTD の MR 画像
　　　前頭葉の限局性の萎縮を認める.

表11　PA の臨床的診断特徴

1. 中核的特徴（すべて必要）
　A. 潜行性に発症し徐々に進行する
　B. 以下のうち少なくとも一つを伴う非流暢性の自発話
　　・失文法
　　・音韻性錯語
　　・失名辞

2. 支持する診断的特徴
　A. 発話と言語
　　・吃／口部失行
　　・復唱障害
　　・失読・失書
　　・早期には語義は障害されない
　　・後期の緘黙
　B. 行動
　　・早期には社会的技能は保たれる
　　・後期には FTD と同様の行動変化を認める
　C. 身体所見
　　・後期の原始反射
　　・無動・固縮・振戦
　D. 検査所見
　　・神経心理学的検査：重度の健忘・空間認知障害を伴わない非流暢性失語
　　・脳波検査：正常か軽度の非対称性徐波化
　　・脳画像検査（形態／機能画像）：優位半球に強い非対称性異常

　b.　進行性非流暢性失語症（progressive non-fluent aphasia：PNFA）

　　左半球シルビウス裂周囲の限局的な変性に伴って文字通り進行性の非流暢性失語が出現する病態である．発語は努力性，プロソディー障害，構音障害を有し，錯語，失名辞，失文法，口部顔面失行を伴うことが多い（表11）．失語症は語想起障害で発症することが多く，音韻性錯語も出現する．復唱の障害，書字障害，計算障害なども加わる．この病態の病理学的特徴は限局性萎縮部位に皮質神経細胞の脱落とグリオーシス，皮質表層の海綿状変化を伴う非特異的変化を認めることが多いが，ピック

病, 皮質基底核変性症, AD, クロイツフェルト-ヤコブ病などの所見を呈することもある. 経過は原因疾患によって異なるが, 典型例では, 失語症から認知症への移行は緩徐で, 明らかな健忘症, 病識の障害, 人格変化が起こるのは末期で, 日常生活活動能力も高いまま維持されやすい.

c. 意味認知症 (semantic dementia: SD)

以前, 側頭葉優位型ピック病と呼ばれていた病態がこれにあたる. 精神行動障害は FTD と同様であるが, 常同症状が単純な動作でなく, 時刻表的行動, それに伴う常同的周遊のようなまとまった行動であることが多い (McMurtray *et al.*, 2006). 時刻表的行動とは細かい日課を自ら決め, その日課通りに生活する強迫・常同症状である. 台風の日でも同じ時間に家を出かけ, 同じコースをたどり, 途中の同じ喫茶店で同じ物を頼み, 同じ時間にそこを出て, 同じコースで帰ってくるというような症状である.

SD の臨床的診断特徴は表 12 のごとくであるが, 初期には語義失語を認める. これは意味記憶障害

表 12　SD の臨床的診断特徴

1. 中核的特徴 (すべて必要)
 A. 潜行性に発症し徐々に進行する
 B-1　以下の特徴を有する言語障害
 ・進行性, 流暢性の空虚な自発話
 ・呼称障害・理解障害で示される語義の障害
 ・意味性錯語
 ・早期からの対人接触の調整障害
 および, または,
 B-2　以下の特徴を有する認知障害
 ・相貌失認
 　および, または,
 ・連合型視覚失認
 C. 知覚的マッチングと模写は可能
 D. 一単語の復唱は可能
 E. 音読・正字法的規則単語の書き取りは可能

2. 支持する診断的特徴
 A. 発話および言語
 ・発話衝動の亢進
 ・独特な語の使用
 ・音韻性錯語の欠如
 ・類音的錯読と錯書
 ・計算能力の保持
 B. 行動
 ・感情移入・共感欠如
 ・狭小化した興味対象
 ・過度の倹約
 C. 身体所見
 ・原始反射は欠如, または後期に出現
 ・無動・固縮・振戦
 D. 検査所見
 ・神経心理学的検査:
 　(a) 呼称・指示の二方向性の障害, および顔と物品の認知障害により示される意味の消失
 　(b) 音韻と統辞, 要素的な認知過程, 空間的技能, 日常生活記憶は保持
 ・脳波検査: 正常
 ・脳画像検査 (形態／機能画像): 著明な側頭葉前方部の異常

が言語の側面にのみ目立っている早期の状態であると考えられる．発語は流暢で構音障害は認めない．復唱，文レベルの了解も良好である．しかし物の名前などの単語の意味がわからなくなる．たとえば，「鉛筆」を眼前に提示して，これは何かと問うてもわからない．語頭音をヒントとして与えても正答を導き出すことは困難である．検者が「えんぴつ」と正答をいっても患者は「聞いたことがない」と回答し，この「えんぴつ」という音に既知感をもたない．場合によっては「えんぴ」と与えた語頭音をその物の名前と思い，「これはえんぴというのですね」と納得する．いくつかの物品を眼前に提示し，その中から「鉛筆」を指示するようにいっても指示できない．すなわち呼称と指示の二方向性の障害を認める．語義失語の段階では，「鉛筆」という名前はわからなくても，鉛筆が何をする物であるかを説明でき，正しく使うこともできる．しかし疾患が進行してくると，「鉛筆」が何をする物であるかがわからなくなり，使用することもできなくなる．またみたことがないといい，視覚的情報からもその物品を同定できなくなる．この段階になると意味記憶障害と判断される．疾患の進行に伴い，既知感をもたず使えない言葉や物品は増えていく．

　SD の典型像は側頭葉優位に楔形の強い限局性の脳萎縮を呈する症例に認められるが，語義失語は左側頭葉優位例で顕著である（図 8）．一方，右側頭葉優位例では，視覚的な情報が喪失されやすく，よくしっているはずの家族や有名人の顔をみても，誰だかわからなくなる．さらに東京タワーなどの有名な建造物もわからず，既知感ももてなくなる．病初期では相貌などの視覚情報からそれを同定することは困難であるが，その人に関する知識や建物についての知識は保持されている．声を聞くと誰であるかわかる．したがってこの段階では連合型視覚失認と考えられるのであるが，疾患の進行に伴い，その人，建物，物品についての情報も失っていき，意味記憶障害のレベルへと至る．
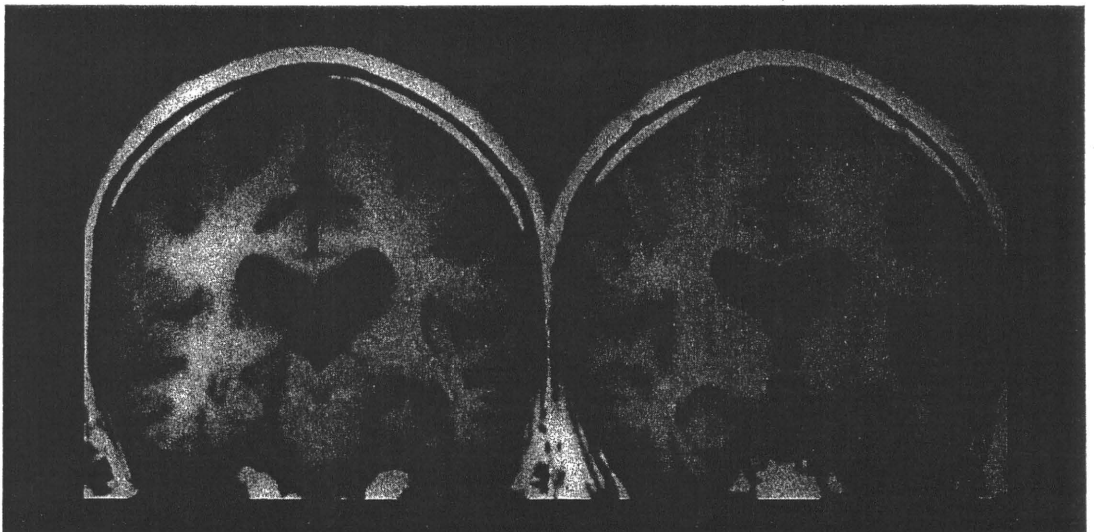


図 8　左側頭葉優位型 SD の MR 画像
　　　左側頭葉，とくに前方部に楔形状の限局性の脳萎縮を認める（右の画像がより前方部の画像）．

### 10.7.3　特発性正常圧水頭症（idiopathic normal pressure hydrocephalus : iNPH）

　正常圧水頭症（normal pressure hydrocephalus : NPH）は Hakim, S. と Adams, R. D. *et al.*（1965）が報告した臨床概念で，古典的には，歩行障害，認知障害，尿失禁の三徴候を有し，脳室拡大はあるが，

**表13 iNPH の診断基準**

I. possible iNPH
  1. 必須項目
    ・60 歳以降の発症
    ・歩行障害, 認知障害, 尿失禁の一つ以上
    ・脳室の拡大 (Evans index>0.3)
    ・髄液圧 < 200 mmH$_2$O, 髄液の性状が正常
    ・他の疾患ですべてを説明できない
    ・脳室拡大をきたす明らかな先行疾患 (くも膜下出血, 髄膜炎, 頭部外傷, 先天性水頭症, 中脳水道狭窄症など) がないか不明
  2. 参考項目
    ・歩行の特徴：小歩, すり足, 不安定, 方向転換時に不安定性が増大, 歩行速度の低下, 歩行時の外股, 後方への易転倒性, 検査時の後方突進現象
    ・緩徐進行性が多いが一時的な進行停止や増悪を認めることもある
    ・他の神経変性疾患・脳疾患の併存はあっても軽度
    ・高位円蓋部脳溝・くも膜下腔の狭小化, シルビウス裂・脳底槽の拡大
    ・periventricular hyperlucency・periventricular hyperintensity の有無は問わない
    ・脳血流検査による他の認知症との鑑別

II. probable iNPH
  1. 必須項目
    ・possible iNPH の必須項目を満たす
    ・以下のいずれかを認める
      (a) CSF タップテストで症状の改善
      (b) CSF ドレナージテストで症状の改善
      (c) 髄液流出抵抗値測定や ICP モニタリングで異常と判定される

III. definite iNPH
  シャント術施行後, 症状の改善を認める

髄液圧は正常範囲内で, 髄液短絡術によって症状が改善する病態である. 先行疾患が明らかでない NPH を iNPH というが, 近年, わが国で行われた地域在住の高齢者を対象にした疫学研究において iNPH は高齢者の 200 人に 1 人の頻度で生じる比較的高頻度の疾患である可能性が指摘され (Iseki *et al.*, 2009), とくに注目されている.

古典的な診断基準ではシャント術を施行しなければ, 診断がつかないことになる. これでは臨床的に使用困難であるため, わが国で作成された iNPH 診療ガイドライン (2004) における診断基準 (表13) では確度の低い順から, possible iNPH, probable iNPH, definite iNPH と段階分けして, シャント術前でも診断可能としている. 三徴と神経画像所見から possible iNPH と診断する. 歩行障害の特徴は, 診断基準の参考項目のごとくである. 認知障害については, 比較的軽症の症例では, 注意機能の障害, 思考速度・反応速度・作業速度の低下, 語想起能力の障害などの前頭葉機能関連障害, および記憶障害を認める. 記憶障害は自ら思い出す再生の障害と比較すると, その刺激があったか否かを判断する再認の障害は軽度である. 排尿障害についてはその内容は尿が貯められなくなる蓄尿症状 (過活動膀胱) が多い. すなわち夜間頻尿, 尿意切迫 (いったん尿意を感じると 5-15 分我慢できない), 切迫性尿失禁, 昼間頻尿を認める. 神経画像学的所見としては, Evans' index (両側側脳室前角間最大幅／その部位における頭蓋内腔幅) >0.3 で表現される脳室の拡大が重要であるが, MRI 冠状断で明らかになる高位円蓋部のくも膜下腔の狭小化も有用な所見である (Kitagaki *et al.*, 1998) (図9). ま
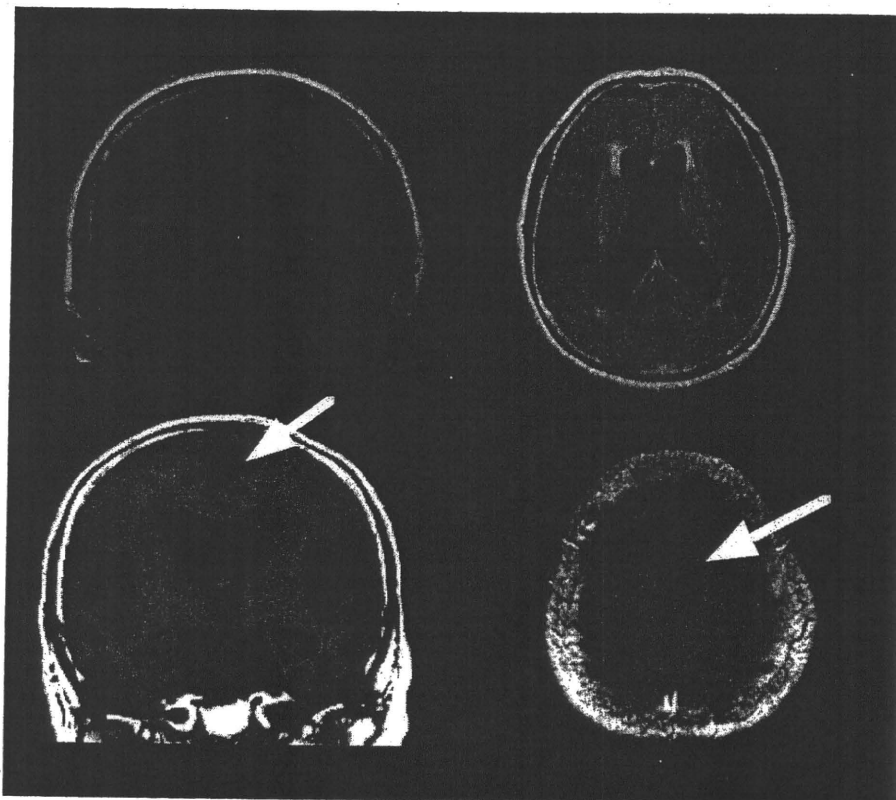
図9　iNPH の MR 画像
　　左上：$T_1$ 強調画像冠状断像. 脳室拡大と高位円蓋部の狭小化を認める.
　　右上：FLAIR 画像水平断像. 側脳室とシルビウス裂の開大を認める.
　　下（矢印部）：局所的な髄液貯留像を認める.

たシルビウス裂の開大, さらに一部の症例では局所的な髄液貯留像を認めることがあり, これも診断に有用である. 上記のような三徴と神経画像所見を呈している患者において, 診断基準に示すような手技で髄液循環不全の存在を明らかにできれば probable iNPH と診断する. そしてシャント術を施行し, その後に症状の改善を確認できたら definite iNPH と診断する.

　シャント術による改善はこれまでの報告をまとめると歩行障害が 58-90%, 認知障害が 29-80%, 排尿障害が 20-78% である. ただし三徴の改善の速度には差があるとされており, 歩行障害と排尿障害は比較的早期に改善するが, 認知障害の改善は遅れる. シャント術の長期効果を調べた研究は少ないが, 少なくとも5年間は非手術群よりも日常生活自立率が高かったと報告されている.

文　献

Aarsland, D. (1999) *J. Neurol. Neurosurg. Psychiatry,* **67**, 492-496.

Adams, R. D., Fisher, C. M., Hakim, S. *et al.* (1965) *N. Engl. J. Med.,* **273**, 117-126.

藍沢鎮雄, 山口弘一, 福井康雄ほか (1985) 老年精神医学 **2**, 365-373.

藍沢鎮雄 (1994) 老年期精神疾患治療のためのストラテジー, 長谷川和夫監, ワールドプランニング, 東京, pp.
　285-304.

Alexopoulos, G. S. (2004) *Late-life Depression,* Oxford University Press, Oxford, p. 24.

Almeida, O. P., Howard, R. J., Levy, R. *et al.* (1995) *Br. J. Psychiatry,* **166**, 215-228.

American Psychiatric Association (1994) *Diagnostic and Statistical Manual of Mental Disorders,* Fourth ed.,
　American Psychiatric Association, Washington D. C. 高橋三郎, 大野裕, 染谷俊幸訳 (1996) DSM-IV 精神疾患

の診断・統計マニュアル，医学書院，東京.

Antithrombic Trialists'Collaboration (2002) *B. M. J.*, **324**, 71-86.

Ariyo, A. A. (2000) *Circulation*, **102**, 1773-1779.

Association Psychiatric World (1999) *Depressin Disorders in Older Person*, NCM Publishers, New York.

Ballard, C., Piggott, M., Johnson, M. *et al.* (2000) *Ann. Neurol.*, **48**, 868-876.

Barnes, D. E. (2006) *Arch. Gen. Psychiatry*, **59**, 273-279.

Boyle, P. A. (2004) *Dement. Geriat. Cogn. Disord.*, **17**, 91-99.

Busse, E. W. and Pfeiffer, E. (1977) *Geriatric Psychiatry, 2nd,* Busse, E. W. and Pfeiffer, E. eds., Little Brown, Boston, pp. 158-211.

Capgras, J. and Reboul-Lachaux, J. (1923) *Bulletin de la Société Clinique de Médicine Mentale*, **2**, 6-16.

Cattell, R. B. (1963) *Psychol. Rev.*, **70**, 1-18.

Chiu, E. (1999) *Depressive Disorders,* John Wiley & Sons (Chichester), pp. 313-363.

Christenson, R. and Blazer, D. (1984) *Am. J. Psychiatry*, **141**, 1088-1091.

Cummings, J. L. (2000) *Neurobiol. Aging*, **21**, 845-861.

Council on scientific affairs (1996) *J. A. M.A.*, **275**, 797-801.

Devanand, D. P. (2002) *Soc. Biol. Psychiatry*, **51** 236-242.

Dubois, B., Feldman, H. H., Jacova, C. *et al.* (2007) *Lancet Neurol.*, **6**, 734-746.

EAFT Study Group (1993) *Lancet*, **342**, 1255-1262.

Edelstyn, N. M. and Oyebode, F. (1999) *Int. J. Geriatr. Psychiatry*, **14**, 48-59.

Ekbom, K. A. (1938) *Acta Psychiatrica et Neurologica Scandinavica*, **13**, 227-259.

Erikson, E. H., Erikson, J. M. and Kivnick, H. Q. (1996) *Vital Involvement in Old Age*, W. W. Nortton & Company, New York.

Erkinjutti, T. (2002) *Lancet*, **359**, 1283-1290.

Evans, M. (1997) *J. Geriatric. Psychiatry*, **12**, 817-824.

Forsen, L. (1999) *J. Epidemiology & Community Health*, **53**, 343-347.

Fukuhara R, Ikeda M, Nebu A. *et al.* (2001) *Neuroreport*, **12**, 2473-2476.

船山道隆 (2006) 老年精神医学雑誌 **17**, 1062-1066.

Gambert, S. R. (1997) *Substance Abuse : A Comprehensive Text Book*, Lowinson, J. H. *et al.* eds., Williams & Wilkins, Baltimore, pp. 692-699.

Goenjian, A. K., Najarian, L. M., Pynoos, R. S. *et al.* (1994) *Am. J. Psychiatry*, **151**, 895-901.

Grady, C. L., Haxby, J. V., Schapiro, M. B. *et al.* (1990) *J. Neuropsychiat. Clin. Neurosci.*, **2**, 373-384.

Hachinski, V. C., Iliff, L. D., Zihka, E. *et al.* (1975) *Arch. Neurol.*, **32**, 632-637.

Harris, M. J., Heaton, R. K., Schalz, A. *et al.* (1997) *Schizophr. Res.*, **27**, 241-248.

平井俊策 (2006) 老年期認知症ナビゲーター，平井俊策監修，メディカルレビュー社，東京.

Hirono, N., Mori, E., Ishii, K., *et al.* (1998) *J. Neuropsychiat. Clin. Neurosci.*, **10**, 433-439.

Holroyd, S., Rabins, P. V., Finkelstein, D. *et al.* (1994) *J. Nerv. Ment. Dis.*, **182**, 273-276.

Horn, J. L. and Cattell, R. B. (1966) *J. Educ. Psychol.*, **57** (5), 253-270.

Horn, J. L. and Cattell, R. B. (1967) *Acta Psychol (Amst).*, **26** (2), 107-129.

Horn, J. L., Cattel, R. B. (1967) *Acta Psychobiologica*, **26**, 107-129.

Howard, R. J., Graham, C., Sham, P. *et al.* (1997) *Br. J. Psychiatry*, **170**, 511-514.

Ikeda, M., Shigenobu, K., Fukuhara, R. *et al.* (2003) *Int. J. Geriatr. Psychiatry*, **18**, 527-532.

池田学 (2004) 高次脳機能研究 **24**, 147-154.

Ikeda, M., Fukuhara, R., Shigenobu, K. *et al.* (2004) *J. Neurol. Neurosurg Psychiatry*, **75**, 146-148.

井野美幸 (2007) 高齢期の心理と臨床心理学，下仲順子編，培風館，東京，pp. 162-170.

Iseki, C., Kawanami, T., Nagasawa, H. *et al.* (2009) *J. Neurol. Sci.*, **277**, 54-57.

Ishii, K., Imamura, T., Sasaki, M. *et al.* (1998) *Neurology*, **51**, 125-130.

Janzarik, W. (1973) *Nervenarzt*, **44**, 515-526.

Jeste, D. V., Lacro, J. P., Gilbert, P. L. *et al.* (1993) *Schizophr. Bull.*, **19**, 817-830.

金子仁郎 (1985) 老人の心理と精神医学，金剛出版，東京，pp. 41-84.

❖❖ Scientific
❖❖ Research

# Restraint-Induced Expression of Endoplasmic Reticulum Stress-Related Genes in the Mouse Brain

Mitsue Ishisaka[1], Takashi Kudo[2], Masamitsu Shimazawa[1], Kenichi Kakefuda[1], Atsushi Oyagi[1], Kana Hyakkoku[1], Kazuhiro Tsuruma[1], Hideaki Hara[1]

[1]Molecular Pharmacology, Department of Biofunctional Evaluation, Gifu Pharmaceutical University; [2]Department of Psychiatry, Osaka University Graduate School of Medicine.
Email: hidehara@gifu-pu.ac.jp

## ABSTRACT

*Depression is a significant public health concern but its pathology remains unclear. Previously, increases in an endoplasmic reticulum (ER) stress-related protein were reported in the temporal cortex of subjects with major depressive disorder who had died by suicide. This finding suggests an association between depression and ER stress. The present study was designed to investigate whether acute stress could affect the ER stress response. Mice were immobilized for a period of 6 hr and then expression of ER stress response-related genes was measured by real-time PCR. We also used enzyme-linked immunosorbent assay for concomitant measurement of the plasma corticosterone levels in the mice. The effect of corticosterone on ER stress proteins was further investigated by treating mice with corticosterone for 2 weeks and then measuring ER protein expression by Western blotting. After a 6 hr restraint stress, mRNA levels of ER stress-related genes, such as the 78-kilodalton glucose regulated protein (GRP78), the 94-kilodalton glucose regulated protein (GRP94), and calreticulin, were increased in the cortex, hippocampus, and striatum of mouse brain. Blood plasma corticosterone level was also increased. In the corticosterone-treated mouse model, the expression of GRP78 and GRP94 was significantly increased in the hippocampus. These results suggest that acute stress may affect ER function and that ER stress may be involved in the pathogenesis of restraint stress, including the development of depression.*

*Keywords*: *Corticosterone, Depression, Endoplasmic Reticulum Stress, Restraint Stress*

## 1. Introduction

Major depression, along with bipolar disorder, has become a common psychiatric disorder in modern society. About 1% of the population is estimated to be affected by major depression one or more times during their lifetime [1]. Even though extensive studies have led to a variety of hypotheses regarding the molecular mechanism underlying depression, the pathogenesis of this disorder remains to be fully elucidated.

The endoplasmic reticulum (ER) is the cell organelle where secretory and membrane proteins are synthesized and folded. It also functions as a $Ca^{2+}$ store and resource of calcium signals. The disturbance of ER functions through events such as disruption of $Ca^{2+}$ homeostasis, inhibition of protein glycosylation or disulfide bond formation, hypoxia and viral or bacterial infection, can result in the accumulation of unfolded or misfolded proteins and may trigger stress responses in the cell (ER stress). To overcome ER stress, an unfolded protein response (UPR) is invoked by the activation of several signaling pathways; this UPR promotes an adaptive response to ER stress and reestablishes homeostasis in the ER [2,3]. Molecular chaperones such as the 78-kilodalton glucose regulated protein (GRP78) and the 94-kilodalton glucose regulated protein are induced and promote correct protein folding. If the damage is too severe to repair, C/EBP-homologous protein (CHOP) and other factors are activated and induce cell apoptosis [4]. On the other hand, if misfolded protein aggregates into insoluble higher-order structures, it can give rise to various diseases. For example, rhodopsin misfolding causes autosomal dominant retinitis pigmentosa [5], while the accumulation of amyloid β-peptide is associated with Alzheimer's disease [6].

*PP*

Some reports have also suggested a relationship between mental disorder and ER stress. In bipolar disorder patients, DNA microarray analysis of cell derived from twins discordant with respect to the disease revealed a down-regulated expression of genes related to ER stress responses such as x-box binding protein 1 (XBP1) and GRP78 [7]. In schizophrenia patients, a similar abnormality of these genes was found [8]. In addition, mood-stabilizing drugs such as valproate and lithium have been reported to increase the expression of GRP78, GRP94, and calreticulin [9]. Similarly, olanzapine, one of the second-generation "atypical" anti-psychotic drugs, appears to potentiates neuronal survival and neural stem cell differentiation by regulation of ER stress response proteins [10].

A recent study reported that significantly increased levels of GRP78, GRP94, and calreticulin were found in the temporal cortex of subjects with major depressive disorder who had died by suicide compared with control subjects who had died of other causes [11]. In addition, hippocampal atrophy [12] and reduction of glial density in the subgenual prefrontal cortex [13] were found in patients with major depression. Stress, a risk factor for depression, has been shown to induce atrophy of the apical dendrites of the hippocampal neurons [14], and to promote neuronal apoptosis in the cerebral cortex [15] in animal depression models. These findings suggest that a stressful situation, which may increase the risk for suicide, serves as an ER stressor. To clarify the relationship between exogenous stress and ER stress, in the present study, we investigated the expression of ER stress-related genes after restraint stress. We also focused on the elevation of corticosterone in the plasma and used a corticosterone-treated depression model to clarify the relationship between chronic corticosterone elevation and ER stress.

## 2. Materials and Methods

### 2.1. Animals

Male 9-week-old ddY mice and male 6-week-old ICR mice (Japan SLC, Hamamatsu, Japan) were used for all experiments. Mice were housed at 24 ± 2°C under a 12 hr light-dark cycle (lights on from 8:00 to 20:00) and had ad libitum access to food and water when not under restraint. Animals were acclimatized to laboratory conditions before the experiment. All procedures relating to animal care and treatment conformed to the animal care guidelines of the Animal Experiment Committee of Gifu Pharmaceutical University. All efforts were made to minimize both suffering and the number of animal used.

### 2.2. Restraint Stress

Male 9-week-old ddY mice (Japan SLC) weighing 30-40

g were used for real-time PCR studies. Mice were placed into 50-mL perforated plastic tubes, which prevented them from turning in any direction. Each mouse was maintained in the tube for 6 hr without any access to food or water.

### 2.3. Sampling

After this restraint stress, a blood sample was collected from the tail and the mouse was decapitated. The brain was quickly removed from the skull, briefly washed in ice-cold saline, and laid on a cooled (4°C) metal plate. The brain was rapidly dissected to separate the hippocampus, striatum, and cortex and stored at -80°C until use.

### 2.4. RNA Isolation

Total RNA was isolated from frozen brain using High Pure RNA Isolation Kit (Roche, Tokyo, Japan). RNA concentrations were determined spectrophotometrically at 260 nm. First-standed cDNA was synthesized in a 20-μl reaction volum using a random primer (Takara, Shiga, Japan) and Moloney murine leukemia virus reverse transcriptase (Invitrogen, Carlsbad, CA, USA).

### 2.5. Reai-Time PCR

Real-time PCR (TaqMan; Applied Biosystems, Foster City, CA, USA) was performed as described previously [16]. Single-standard cDNA was synthesized from total RNA using a high capacity cDNA archive kit (Applied Biosystems). Quantitative real-time PCR was performed using a sequence detection system (ABI PRISM 7900HT; Applied Biosystems) with a PCR master mix (TaqMan Universal PCR Master Mix; Applied Biosystems), according to the manufacturer's protocol. A gene expression product (Assays-on-Demand Gene Expression Product; Applied Biosystems) was used for measurements of mRNA expression by real-time PCR. The primers used for amplification were as follows: GRP78: 5'-GTTTG CTGAGGAAGACAAAAAGCTC-3' and 5'-CACTTCC ATAGAGTTTGCTGATAATTG-3'; CHOP: 5'-GGAG CTGGAAGCCTGGTATGAGG-3' and 5'-TCCCTGGT CAGGCGCTCGATTTCC-3'; GRP94: 5'-CTCACCATT TGGATCCTGTGTG-3' and 5'-CACATGACAAGATT TTACATCAAGA-3'; calreticulin: 5'-GCCAAGGACG AGCTGTAGAGAG-3' and 5'-GGTGAGGGCTGAAG GAGAATC-3'; ERdj4: 5'-TCTAGAATGGCTACTCCC CAGTCAATTTTC-3' and 5'-TCTAGACTACTGTCCT GAACAGTCAGTG-3'; EDEM: 5'-TGGGTTGGAAAG CAGAGTGGC-3' and 5'-TCCATTCCTACATGGAGG TAG-3'; p58IPK 5'-GAGGTTTGTGTTTGGGATGCAG- 3' and 5'-GCTCTTCAGCTGACTCAATCAG-3'; ASNS: 5'-AGGTTGATGATGCAATGATGG-3' and 5'-TCCC CTATCTACCCACAGTCC-3'; β-actin: 5'-TCCTCCCT

GGAGAAGAGCTAC-3' and 5'-TCCTGCTTGCTGAT CCACAT-3' The thermal cycler conditions were as follows: 2 min at 50°C and then 10 min at 95°C, followed by two-step PCR for 50 cycles consisting of 95°C for 15s followed by 60°C for 1 min. For each PCR measurement, we checked the slope value, $R^2$ value, and linear range of a standard curve of serial dilutions. All reactions were performed in duplicate. The results were expressed relative to a β-actin internal control.

## 2.6. Measurement of Plasma Corticosterone

Plasma was obtained as described previously [17] and the concentration of corticosterone was determined *via* a corticosterone EIA kit (Assay Designs, Inc., Ann Arbor, MI, USA) according to the manufacturer's protocol.

## 2.7. Chronic Corticosterone Treatment

Male 6-week-old ICR mice (Japan SLC) weighing 20-25 g were used for chronic oral corticosterone exposure as described in a previous report [18]. Briefly, corticosterone (25 µg/mL free base; 4-pregnen-11β 21-DIOL-3 20-DIONE 21-hemisuccinate; Steraloids, Inc., RI, USA) was add to tap water and the pH was brought to 12-13 with 10 N NaOH (Kishidai Chemical, Osaka, Japan), followed by stirring at 4°C until dissolved (3 to 7 hr). Following dissolution, the pH was brought to 7.0-7.4 with 10 N HCl (Wako, Osaka, Japan). Group-housed ICR mice were presented with this corticosterone solution in place of normal drinking water for 14 days, resulting in a dose of approximately 8.7 mg/kg/day (p.o). Animals were weaned with 3 days of 12.5 µg/mL, and then 3 days with 6.25 µg/mL, to allow for gradual recovery of endogenous corticosterone secretion.

## 2.8. Western Blot Analysis

At 35 days, each mouse was decapitated and its brain was quickly removed from the skull, briefly washed in ice-cold saline, and laid on a cooled (4°C) metal plate. The brain was rapidly dissected to separate the hippocampus and stored at -80°C until use. Brain samples were homogenized in 10 mL/g tissue ice-cold lysis buffer [50 mM Tris-HCl (pH 8.0) containing 159 mM NaCl, 50 mM EDTA, 1% Triton X-100, and protease/phosphatase inhibitor mixture] using a homogenizer (Physcotron; Microtec Co. Ltd., Chiba, Japan). Lysates were centrifuged at 12,000×g for 15 min at 4°C. Supernatants were collected and boiled for 5 min in SDS sample buffer (Wako). Equal amounts of protein were subjected to 10% SDS-PAGE gradient gel and then transferred to poly (vinylidene difluoride) membranes (Immobilon-P; Millipore, MA, USA). After blocking with Block Ace (Snow Brand Milk Products Co. Ltd., Tokyo, Japan) for 30 min, the membranes were incubated with primary antibody. The primary antibodies used were as follows: mouse anti-BiP antibody (BD Bioscience, CA, USA) for GRP78, mouse anti-KDEL antibody (Stressgen Bioreagents Limited Partnership, B.C., Canada) for GRP94, and mouse anti-actin antibody (Sigma-Aldrich, St. Louis, MO, USA). Subsequently, the membrane was incubated with the secondary antibody [goat anti-mouse (Pierce Biotechnology, IL, USA)]. The immunoreactive bands were visualized using Super Signal West Femto Maximum Sensitivity Substrate (Pierce Biotechnology) and then measured using LAS-4000 mini (Fujifilm, Tokyo, Japan).

## 2.9. Statistical Analysis

Statistical comparisons were made by Student's *t*-test using Statview version 5.0 (SAS Institute Inc., NC, USA), with $p < 0.05$ being considered statistically significant.

## 3. Results and Discussion

Real-time PCR was carried out to investigate whether the expression of ER stress response-related genes in the brain was changed by 6-hr restraint stress. In this study, we investigated the expression of GRP94, carleticulin, ER degradation-enhancing α-mannosidase-like protein (EDEM), protein kinase inhibitor of 58 kDa (p58[IPK]), asparagines synthetase (ASNS), GRP78, ER-localized DnaJ 4 (ERdj4), and C/EBP homologous protein (CHOP). The expression of GRP78, GRP94, and calreticulin mRNA was significantly increased in the hippocampus, striatum, and cortex (**Figure 1**). In addition, there was significantly increased expression of p58[IPK] mRNA in the cortex, but not in the hippocampus or striatum.

We next investigated whether restraint stress affected the plasma concentrations of corticosterone, as previously reported. Immediately following the 6-hr restraint stress, significantly higher plasma corticosterone concentrations were found in stressed mice compared to unstressed mice. Seven days after the restraint stress, the plasma corticosterone recovered to the normal control level (**Figure 2**).

To clarify the mechanism of ER stress-related mRNA elevation, we artificially elevated the plasma concentrations of corticosterone in mice for 2 weeks and then measured the levels of ER stress-related proteins. In the corticosterone-treated animal model, the expression of GRP78 and GRP94 in the hippocampus was significantly increased compared to control levels (**Figure 3**).

Restraint stress is used widely to induce stress responses in animals, and it is known that a number of stresses, including restraint stress, can cause depression in animals. In the present study, we found that several ER stress-related genes were increased in the mouse hippocampus, striatum, and cortex after restraint stress.

(a)

(b)

(c)
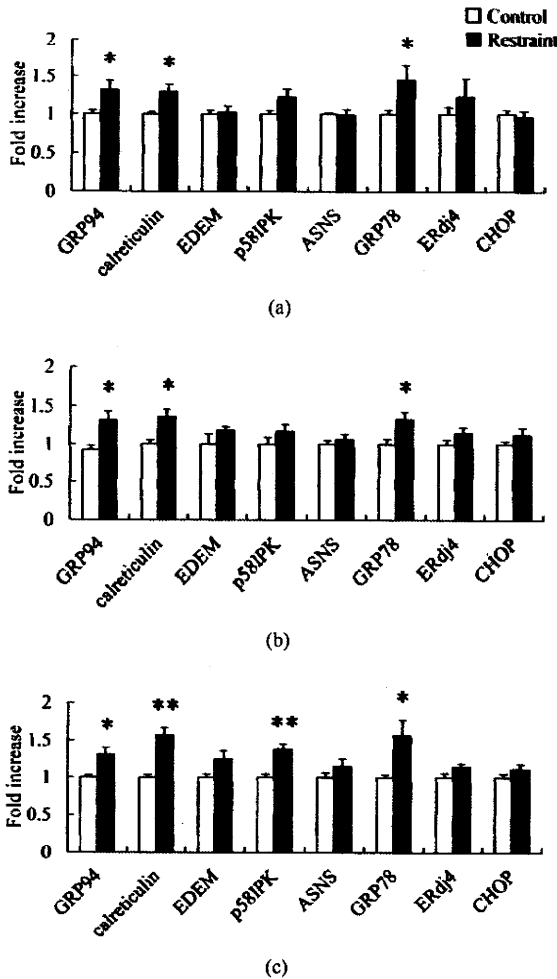
Figure 1. The expression mRNA of ER stress-related factors in the mouse brain after 6 hr restraint-stress. Mice were immobilized for 6 hr in a 50-mL perforated plastic tube. White and black bars represent the control group and the restraint group, respectively. Immediately after restraint, mice were killed and real-time PCR was performed on brain tissues from the (a) hippocampus, (b) striatum, and (c) cortex. Data represent means and S.E.M., n = 3 to 5. *p < 0.05, **p < 0.01 vs. control group. GRP94: the 94-kilodalton glucose regulated protein, EDEM: ER degradation-enhancing α-mannosidase-like protein, p58IPK: protein kinase inhibitor of 58 kilodalton, ASNS: asparagines synthetase, GRP78: the 78-kilodalton glucose regulated protein, ERdj4: ER-localized DnaJ 4, CHOP: C/EBP-homologous protein.

The significant increases in expression of GRP78, GRP94, and calreticulin agreed with the findings of a previous report of changes in the temporal cortex of subjects with major depression who died by suicide [11]. However, no study has yet specifically investigated expression changes of these genes in the hippocampus or the striatum in subjects with depression.
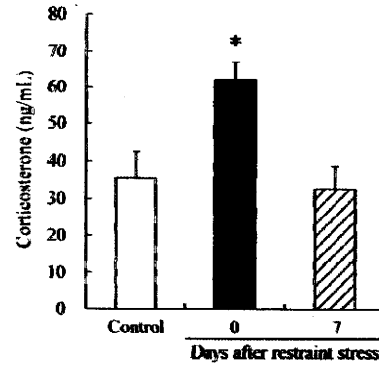


Figure 2. The effect of 6 hr restraint stress on the concentration of corticosterone in mouse plasma. Mice were immobilized for 6 hr. Immediately after restraint and 7 days later, blood samples were collected and concentration of plasma corticosterone was measured by ELISA. Restraint stress significantly increased the concentration of corticosterone in plasma. The corticosterone levels decreased to the normal control levels 7 days after restraint stress. Data represent means and S.E.M., n = 7. *p < 0.05 vs. control group.

GRP78, otherwise known as BiP, is one of the best-characterized ER chaperone proteins and is regarded as a classical marker of UPR activation. Overexpression of GRP78 has been reported to inhibit the upregulation of CHOP, which plays a key role in regulating cell growth and which has been implicated in apoptosis [19,20]. GRP94 and calreticulin are also ER chaperone proteins and show protective effects against ER stress [21]. The increase in these chaperones after restraint stress (Figure 1) may represent an attempt to oppose the toxic effect of prolonged stress and the high concentrations of glucocorticoid, such as corticosterone, on the brain. Dysregulation of the hypothalamic-pituitary-adrenal (HPA) axis, which controls glucocorticoid levels, has been reported in most depression patients and glucocorticoid level of depression patients was higher than those of normal ones [22-24]. In the mice in the present study, 6-hr restraint stress elevated the concentration of corticosterone in plasma, suggesting that restraint stress induced a response similar to depression.

Recently, corticosterone has been reported to exert immunostimulatory effects on macrophages via induction of ER stress [25]. Following corticosterone treatment, the glucocorticoid receptor (GR) binds onto B-cell lymphoma 2 (Bcl-2), a protein that affects cytochrome C and calcium release from mitochondria. Subsequently, this GR/Bcl-2 complex moves into mitochondria and regulates mitochondrial functions in an inverted "U"-shaped manner–i.e., a high dose treatment with corticosterone decreased levels of GRs and Bcl-2 in mitochondria and intracellular calcium was increased [26,27]. Substances
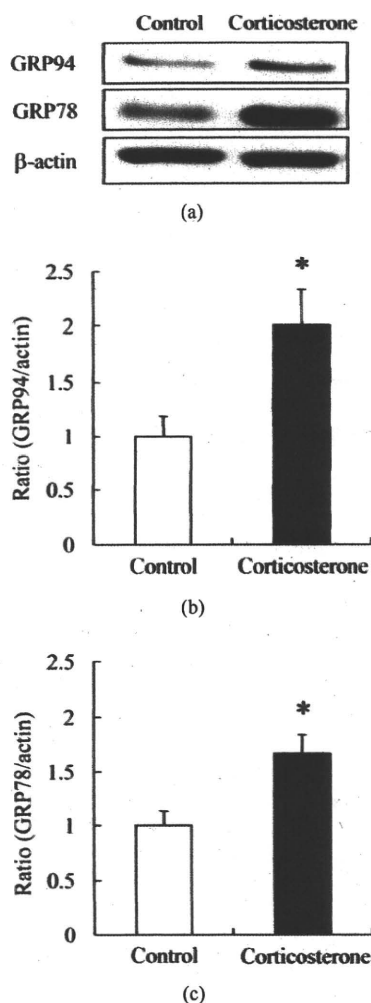
**Figure 3. The expression of GRP78 and GRP94 in the hippocampus in a mouse model of chronic corticosterone induced depression. (a) Representative band images show immunoreactivities against GRP94, GRP78, and β-actin. (b) GRP78 expression was significantly increased by corticosterone exposure. (c) GRP94 expression was also increased by corticosterone exposure. Data represent means and S.E.M., n = 5 or 6. \*p < 0.05 vs. control group.**

that deplete the ER $Ca^{2+}$ stores, such as thapsigargin, are widely used an ER stressors. Therefore, elevation of $Ca^{2+}$ via GR may be sufficient for control of ER stress responses. In the present study, the restraint stress induced the expressions of only GRP78, GRP94, and calreticulin, but not other ER proteins. GRP78, GRP94, and calreticulin function as $Ca^{2+}$ binding proteins [28]. Under the high concentration of corticosterone, the intracellular $Ca^{2+}$ level might be higher, therefore, the expressions of GRP78, GRP94, and calreticulin might be increased.

Intracerebroventricular administration of thapsigargin has been reported to produce a depressant-like behavior

[29]. A 14-days corticosterone treatment has also shown to induce depression symptoms in mice [18]. We used this animal model to investigate the effect of chronic elevation of corticosterone on ER stress responses in brain. As expected, significant increases in GRP78 and GRP94 proteins were observed in the hippocampus (**Figure 3**). The increase of GRP78 was consistent with the result of a previous report [30]. On the other hand, no change in these proteins was observed in the cortex (data not shown). Mineralocorticoid receptor (MR) and GR, which are the targets of corticosterone, are known to be well expressed in the hippocampus [31,32]. These reports, together with our findings, indicate that the hippocampus may be more sensitive to corticosterone exposure than are other brain regions. Many reports have referred to hippocampal atrophy in patients with depression [12,14]. In the cortex, it had been reported that chronic stress increased the caspase-3 positive neurons, in other words, exogenous stress was contributing to the cell apoptosis [15]. In our study, corticosterone exposure was performed for 2 weeks, but, in fact, long-term cortisol elevation has been observed in most depression patients. More extended corticosterone treatment may affect the expression of ER stress proteins in the cortex.

Recently, many experiments have focused on the relationship between depression and neurogenesis. Interestingly, ER stress also affects adult neurogenesis in the brain [33]. Brain-derived neurotrophic factor (BDNF), which promotes neurogenesis, is also known to inhibit neuronal cell death induced by ER stress [34]. These reports may also point to an involvement of ER stress in depression.

## 4. Conclusions

Restraint stress, which may contribute to depression in mice, may up-regulate the ER stress response via corticosterone elevation. This suggests the possibility of an ER stress involvement in the pathogenesis of stress-related depression disorders.

## REFERENCES

[1]   R. C. Kessler, P. Berglund, O. Demler, R. Jin, K. R. Me-rikangas and E. E. Walters, "Lifetime Prevalence and Age-of-onset Distributions of DSM-IV Disorders in the National Comorbidity Survey Replication," *Archives of general psychiatry*, Vol. 62, No. 6, 2005, pp. 593-602. doi:10.1001/archpsyc.62.6.593

[2]   D. Ron and P. Walter, "Signal Integration in the Endoplasmic Reticulum Unfolded Protein Response," *Nature reviews*, Vol. 8, No. 7, 2007, pp. 519-529.

[3]   V. I. Rasheva and P. M. Domingos, "Cellular Responses to Endoplasmic Reticulum Stress and Apoptosis," *Apoptosis*, Vol. 14, No. 8, 2009, pp. 996-1007.

*PP*

doi:10.1007/s10495-009-0341-y

[4]  S. Oyadomari and M. Mori, "Roles of CHOP/GADD153 in Endoplasmic Reticulum Stress," *Cell Death and Differentiation*, Vol. 11, No. 4, 2004, pp. 381-389. doi:10.1038/sj.cdd.4401373

[5]  R. S. Saliba, P. M. Munro, P. J. Luthert and M. E. Chee-tham, "The Cellular Fate of Mutant Rhodopsin: Quality Control, Degradation and Aggresome Formation," *Journal of cell science*, Vol. 115, No. Pt 14, 2002, pp. 2907-2918.

[6]  E. H. Koo, P. T. Lansbury, Jr. and J. W. Kelly, "Amyloid Diseases: Abnormal Protein Aggregation in Neurodegen-era-tion," *Proceedings of the National Academy of Sciences of the United States of America*, Vol. 96, No. 18, 1999, pp. 9989-9990. doi:10.1073/pnas.96.18.9989

[7]  C. Kakiuchi, K. Iwamoto, M. Ishiwata, M. Bundo, T. Kasahara, I. Kusumi, T. Tsujita, Y. Okazaki, S. Nanko, H. Kunugi, T. Sasaki and T. Kato, "Impaired Feedback Regulation of XBP1 as a Genetic Risk Factor for Bipolar disorder," *Nature Genetics*, Vol. 35, No. 2, 2003, pp. 171-175. doi:10.1038/ng1235

[8]  C. Kakiuchi, M. Ishiwata, T. Umekage, M. Tochigi, K. Kohda, T. Sasaki and T. Kato, "Association of the XBP1-116C/G Polymorphism with Schizophrenia in the Japanese Population," *Psychiatry and Clinical Neurosciences*, Vol. 58, No. 4, 2004, pp. 438-440. doi:10.1111/j.1440-1819.2004.01280.x

[9]  L. Shao, X. Sun, L. Xu, L. T. Young and J. F. Wang, "Mood Stabilizing Drug Lithium Increases Expression of Endoplasmic Reticulum Stress Proteins in Primary Cultured Rat Cerebral Cortical Cells," *Life Sciences*, Vol. 78, No. 12, 2006, pp. 1317-1323. doi:10.1016/j.lfs.2005.07.007

[10] S. Kurosawa, E. Hashimoto, W. Ukai, S. Toki, S. Saito and T. Saito, "Olanzapine Potentiates Neuronal Survival and Neural Stem Cell Differentiation: Regulation of Endo-plasmic Reticulum Stress Response Proteins," *Journal of Neural Transmission*, Vol. 114, No. 9, 2007, pp. 1121-1128. doi:10.1007/s00702-007-0747-z

[11] C. Bown, J. F. Wang, G. MacQueen and L. T. Young, "Increased Temporal Cortex ER Stress Proteins in Depressed Subjects Who Died by Suicide," Neuropsycho-pharmacology, Vol. 22, No. 3, 2000, pp. 327-332. doi:10.1016/S0893-133X(99)00091-3

[12] Y. I. Sheline, P. W. Wang, M. H. Gado, J. G. Csernansky and M. W. Vannier, "Hippocampal Atrophy in Recurrent Major Depression," *Proceedings of the National Academy of Sciences of the United States of America*, Vol. 93, No. 9, 1996, pp. 3908-3913. doi:10.1073/pnas.93.9.3908

[13] D. Ongur, W. C. Drevets and J. L. Price, "Glial Reduction in the Subgenual Prefrontal Cortex in Mood Disorders," *Proceedings of the National Academy of Sciences of the United States of America*, Vol. 95, No. 22, 1998, pp. 13290-13295. doi:10.1073/pnas.95.22.13290

[14] Y. Watanabe, E. Gould and B. S. McEwen, "Stress Induces Atrophy of Apical Dendrites of Hippocampal CA3 Pyramidal Neurons," *Brain research*, Vol. 588, No. 2,

1992, pp. 341-345. doi:10.1016/0006-8993(92)91597-8

[15] A. Bachis, M. I. Cruz, R. L. Nosheny and I. Mocchetti, "Chronic Unpredictable Stress Promotes Neuronal Apoptosis in the Cerebral Cortex," *Neuroscience Letters*, Vol. 442, No. 2, 2008, pp. 104-108. doi:10.1016/j.neulet.2008.06.081

[16] D. Chen, E. Padiernos, F. Ding, I. S. Lossos and C. D. Lopez, "Apoptosis-stimulating Protein of P53-2 (ASPP2/53BP2L) is an E2F Target Gene," *Cell Death and Differentiation*, Vol. 12, No. 4, 2005, pp. 358-368. doi:10.1038/sj.cdd.4401536

[17] O. I. Abatan, K. B. Welch and J. A. Nemzek, "Evaluation of Saphenous Venipuncture and Modified Tail-clip Blood Collection in Mice," *Journal of the American Association for Laboratory Animal Science,*, Vol. 47, No. 3, 2008, pp. 8-15.

[18] S. L. Gourley and J. R. Taylor, "Recapitulation and Reversal of a Persistent Depression-like Syndrome in Rodents," *Current Protocols in Neuroscience* Chapter 9, 2009, Unit-9.32.

[19] X. Z. Wang, B. Lawson, J. W. Brewer, H. Zinszner, A. Sanjay, L. J. Mi, R. Boorstein, G. Kreibich, L. M. Hendershot and D. Ron, "Signals from the Stressed Endoplasmic Reticulum Induce C/EBP-homologous Protein (CHOP/GADD153)," *Molecular and Cellular Biology*, Vol. 16, No. 8, 1996, pp. 4273-4280.

[20] H. Zinszner, M. Kuroda, X. Wang, N. Batchvarova, R. T. Lightfoot, H. Remotti, J. L. Stevens and D. Ron, "CHOP is Implicated in Programmed Cell Death in Response to Impaired Function of the Endoplasmic Reticulum," *Genes & Development*, Vol. 12, No. 7, 1998, pp. 982-995. doi:10.1101/gad.12.7.982

[21] M. Cechowska-Pasko, "Endoplasmic Reticulum Chaperons," *Postepy Biochemii*, Vol. 55, No. 4, 2009, pp. 416-424.

[22] C. A. Sandman, J. L. Barron and L. Parker, "Disregulation of Hypothalamic-pituitary-adrenal Axis in the Mentally Retarded," *Pharmacology, Biochemistry, and Behavior*, Vol. 23, No. 1, 1985, pp. 21-26. doi:10.1016/0091-3057(85)90124-8

[23] A. Roy, "Hypothalamic-pituitary-adrenal Axis Function and Suicidal Behavior in Depression," Biological psychiatry, Vol. 32, No. 9, 1992, pp. 812-816. doi:10.1016/0006-3223(92)90084-D

[24] J. F. Lopez, D. M. Vazquez, D. T. Chalmers and S. J. Watson, "Regulation of 5-HT Receptors and the Hypothalamic-pituitary-adrenal Axis. Implications for the Neurobiology of Suicide," *Annals of the New York Academy of Sciences*, Vol. 836, No. 1, 1997, pp. 106-134.

[25] J. Y. Zhou, H. J. Zhong, C. Yang, J. Yan, H. Y. Wang and J. X. Jiang, "Corticosterone Exerts Immunostimulatory Effects on Macrophages via Endoplasmic Reticulum Stress," *The British Journal of Surgery*, Vol. 97, No. 2, 2010, pp. 281-293. doi:10.1002/bjs.6820

[26] J. Du, B. McEwen and H. K. Manji, "Glucocorticoid Receptors Modulate Mitochondrial Function: A Novel Mechanism for Neuroprotection," *Communicative & In-*

*PP*

*tegrative Biology*, Vol. 2, No. 4, 2009, pp. 350-352.

[27] J. Du, Y. Wang, R. Hunter, Y. Wei, R. Blumenthal, C. Falke, R. Khairova, R. Zhou, P. Yuan, R. Machado-Vieira, B. S. McEwen and H. K. Manji, "Dynamic Regulation of Mitochondrial Function by Glucocorticoids," *Proceedings of the National Academy of Sciences of the United States of America*, Vol. 106, No. 9, 2009, pp. 3543-3548. doi:10.1073/pnas.0812671106

[28] H. Coe and M. Michalak, "Calcium Binding Chaperones of the Endoplasmic Reticulum," *General Physiology and Biophysics*, Vol. 28 Spec No Focus, 2009, pp. 96- 103.

[29] N. Galeotti, A. Bartolini and C. Ghelardini, "Blockade of Intracellular Calcium Release Induces an Antidepressant-like Effect in the Mouse Forced Swimming Test," *Neuropharmacology*, Vol. 50, No. 3, 2006, pp. 309-316. doi:10.1016/j.neuropharm.2005.09.005

[30] S. L. Gourley, F. J. Wu, D. D. Kiraly, J. E. Ploski, A. T. Kedves, R. S. Duman and J. R. Taylor, "Regionally Specific Regulation of ERK MAP Kinase in a Model of Antidepressant-sensitive Chronic Depression," Biological psychiatry, Vol. 63, No. 4, 2008, pp. 353-359.

doi:10.1016/j.biopsych.2007.07.016

[31] T. Ito, N. Morita, M. Nishi and M. Kawata, "In Vitro and in Vivo Immunocytochemistry for the Distribution of Mineralocorticoid Receptor with the Use of Specific Antibody," *Neuroscience Research*, Vol. 37, No. 3, 2000, pp. 173-182. doi:10.1016/S0168-0102(00)00112-7

[32] F. Han, H. Ozawa, K. Matsuda, M. Nishi and M. Kawata, "Colocalization of Mineralocorticoid Receptor and Glucocorticoid Receptor in the Hippocampus and Hypothalamus," *Neuroscience Research*, Vol. 51, No. 4, 2005, pp. 371-381. doi:10.1016/j.neures.2004.12.013

[33] P. J. Lucassen, W. Scheper and E. J. Van Someren, "Adult Neurogenesis and the Unfolded Protein Response; New Cellular and Molecular Avenues in Sleep Research," *Sleep Medicine Reviews*, Vol. 13, No. 3, 2009, pp. 183-186. doi:10.1016/j.smrv.2008.12.004

[34] G. Chen, Z. Fan, X. Wang, C. Ma, K. A. Bower, X. Shi, Z. J. Ke and J. Luo, "Brain-derived Neurotrophic Factor Suppresses Tunicamycin-induced Upregulation of CHOP in Neurons," *Journal of Neuroscience Research*, Vol. 85, No. 8, 2007, pp. 1674-1684. doi:10.1002/jnr.21292

*PP*

# ENU-induced missense mutation in the C-propeptide coding region of *Col2a1* creates a mouse model of platyspondylic lethal skeletal dysplasia, Torrance type

Tatsuya Furuichi · Hiroshi Masuya · Tomohiko Murakami · Keiichiro Nishida ·
Gen Nishimura · Tomohiro Suzuki · Kazunori Imaizumi · Takashi Kudo ·
Kiyoshi Ohkawa · Shigeharu Wakana · Shiro Ikegawa

**Abstract** The *COL2A1* gene encodes the $\alpha1$(II) chain of the homotrimeric type II collagen, the most abundant protein in cartilage. In humans, *COL2A1* mutations create many clinical phenotypes collectively termed type II collagenopathies; however, the genetic basis of the phenotypic diversity is not well elucidated. Therefore, animal models corresponding to multiple type II collagenopathies are required. In this study we identified a novel *Col2a1* missense mutation—c.44406A>C (p.D1469A)—produced by large-scale *N*-ethyl-*N*-nitrosourea (ENU) mutagenesis in a mouse line. This mutation was located in the C-propeptide coding region of *Col2a1* and in the positions corresponding to a human *COL2A1* mutation responsible for platyspondylic lethal skeletal dysplasia, Torrance type (PLSD-T). The phenotype was inherited as a semidominant trait. The heterozygotes were mildly but significantly smaller than wild-type mice. The homozygotes exhibited lethal skeletal dysplasias, including extremely short limbs, severe spondylar dysplasia, severe pelvic hypoplasia, and brachydactyly. As expected, these skeletal defects in the homozygotes were similar to those in PLSD-T patients. The secretion of the mutant proteins into the extracellular space was disrupted, accompanied by abnormally expanded rough endoplasmic

T. Furuichi (✉) · K. Ohkawa
Laboratory Animal Facility, Research Center for Medical Sciences, Jikei University School of Medicine,
3-25-8 Nishi-shinbashi, Minato-ku, Tokyo 105-8461, Japan
e-mail: furuichi@jikei.ac.jp

T. Furuichi · S. Ikegawa
Laboratory for Bone and Joint Diseases,
Center for Genomic Medicine, RIKEN, 4-6-1 Shirokanedai,
Minato-ku, Tokyo 108-8639, Japan

H. Masuya
Technology and Development Unit for Knowledge Base
of Mouse Phenotype, RIKEN Bioresource Center,
3-1-1 Koyadai, Tsukuba, Ibaraki 305-0074, Japan

T. Murakami
Division of Molecular and Cellular Biology, Department
of Anatomy, Faculty of Medicine, University of Miyazaki,
5200 Kihara, Kiyotake, Miyazaki 889-1692, Japan

K. Nishida
Department of Human Morphology, Okayama University
Graduate School of Medicine, Dentistry and Pharmaceutical
Sciences, 2-5-1 Shikata-cho, Okayama 700-8558, Japan

G. Nishimura
Department of Pediatric Imaging, Tokyo Metropolitan
Children's Medical Center, 2-8-9 Musashidai, Futyu,
Tokyo 183-8561, Japan

T. Suzuki · S. Wakana
Technology and Development Team for Mouse Phenotype
Analysis, Japan Mouse Clinic, RIKEN Bioresource Center,
3-1-1 Koyadai, Tsukuba, Ibaraki 305-0074, Japan

K. Imaizumi
Department of Biochemistry, Graduate School of Biomedical
Science, Hiroshima University, 1-2-3 Kasumi, Minami-ku,
Hiroshima 734-8553, Japan

T. Kudo
Department of Psychiatry and Behavioral Science,
Osaka University Graduate School of Medicine,
2-2 Yamadaoka, Suita, Osaka 565-0871, Japan

<span style="float:right">🙋 Springer</span>

reticulum (ER) and upregulation of ER stress-related genes, such as *Grp94* and *Chop*, in chondrocytes. These findings suggested that the accumulation of mutant type II collagen in the ER and subsequent induction of ER stress are involved, at least in part in the PLSD-T–like phenotypes of the mutants. This mutant should serve as a good model for studying PLSD-T pathogenesis and the mechanisms that create the great diversity of type II collagenopathies.

## Introduction

Type II collagen is the most abundant protein in cartilage and, along with other tissue-specific collagens and proteoglycans, provides structural integrity to tissue (Myllyharju and Kivirikko 2004; Olsen 1995). This fibrillar collagen is a homotrimer composed of three collagen α1(II) chains containing segments with a characteristic Gly-X-Y repeat sequence that forms a triple-helical structure. As with other fibrillar collagen chains, these chains are synthesized as procollagen, which contains noncollagenous domains at both the N- and C-termini. The C-terminal noncollagenous domain, termed C-propeptide, is essential for triple-helical formation (Doege and Fessler 1986; Khoshnoodi et al. 2006). After being secreted into the extracellular space, the noncollagenous domains of both ends are cleaved by specific proteinases.

*COL2A1* encodes the collagen α1(II) chain, and in humans, heterozygous mutations in this gene lead to many clinical phenotypes collectively termed type II collagenopathies (Kuivaniemi et al. 1997; Nishimura et al. 2005). Most *COL2A1* mutations have been identified in the coding region of the triple-helical domain. Truncation mutations in this region produce Sticker dysplasia type-I (STD-I) or Kniest dysplasia (KND) (Ahmad et al. 1991; Winterpacht et al. 1993), and missense mutations cause a spectrum of spondyloepiphyseal dysplasia (SED) or hypochondrogenesis (HCG) (Korkko et al. 2000; Nishimura et al. 2005). Mutations in the C-propeptide coding region are not common and produce variable clinical phenotypes such as platyspondylic lethal skeletal dysplasia, Torrance type (PLSD-T) (Nishimura et al. 2004; Zankl et al. 2005), spondyloperipheral dysplasia (SPPD) (Zabel et al. 1996), SED congenital (SEDC) (Unger et al. 2001), and HCG (Mortier et al. 2000).

The disproportionate micromelia (*Dmm*) mouse, generated by radiation-induced mutagenesis, is the only known example of an animal model possessing endogenous mutations in the C-propeptide coding region of *Col2a1* (Brown et al. 1981; Pace et al. 1997). A 3-bp deletion, substituting Lys and Thr with Asn (p.K1448_T1449delinsN), was identified in this mutant (Pace et al. 1997). The

homozygotes have severe skeletal dysplasia and die at birth because of thoracic insufficiency. The heterozygotes appear normal at birth, exhibit only a mild dwarfism beginning at 1 week of age, and develop early-onset osteoarthritis (OA) that becomes conspicuous at 3 months of age (Bomsta et al. 2006). To understand at the molecular level the phenotypic diversity of type II collagenopathies with C-propeptide mutations, additional animal models corresponding to PLSD-T, SPPD, SEDC, and HGG phenotypes are required.

In this study we identified a novel *Col2a1* mouse mutant carrying a missense mutation in the C-propeptide coding region that was produced by a large-scale *N*-ethyl-*N*-nitrosourea (ENU) mutagenesis program (Inoue et al. 2004; Masuya et al. 2005a, b, 2007). The amino acid residue resulting from this mutation corresponded to that of human *COL2A1* mutations responsible for PLSD-T. As expected, the skeletal defects of the homozygous mice were similar to those of PLSD-T patients. This mouse will be a good tool for studying PLSD-T pathogenesis and the mechanisms that create the great diversity of type II collagenopathies.

## Materials and methods

### ENU mutagenesis, inheritance testing, and gene mapping

The method for mouse ENU mutagenesis is available at http://www.brc.riken.go.jp/lab/gsc/mouse/ and in previous reports (Inoue et al. 2004; Masuya et al. 2005a, b, 2007). C57BL/6J and DBA/2J mice were purchased from CLEA Japan (Tokyo, Japan). C57BL/6J males administered ENU (total dosage of 150–250 mg/kg) were crossed to DBA/2J females. The resultant F1 hybrids (G1 animals) were subjected to screening for various phenotypes at 8 weeks of age. Examination of adult limb phenotype was performed as a subtest of the modified-SHIRPA protocol, a comprehensive package of screens for morphological and behavioral phenotypes (Masuya et al. 2005a). A complete list of the subtests is available at the above website. M100856 mouse lines were crossed with wild-type DBA/2J mice to test for phenotype transmission and for genetic mapping of the causative genes. Genomic DNA was prepared from the tail tips of the G2 progeny using the NA-2000 automatic nucleic acid isolation system (KURABO, Osaka, Japan). We used the db-SNP website (http://www.ncbi.nlm.nih.gov/entrez/query.fcgi?db=snp) for single nucleotide polymorphisms (SNPs) and the microsatellite markers listed on the MGI website (http://www.informatics.jax.org/) for simple sequence length polymorphisms. Polymorphic loci were examined using TaqMan MGB assays on the ABI

7700 and ABI 7900 Sequence Detection Systems (Applied Biosystems, Foster City, CA, USA).

## Mutation screening and genotyping

We searched for *Col2a1* mutations using cDNAs derived from M100856 lines. We amplified by PCR seven overlapping cDNA fragments that cover the entire coding region and sequenced the PCR products with an ABI 3700 automated sequencer (Applied Biosystems). PCR conditions and primer sequences are available upon request. For the mutation numbering, +1 corresponds to the A of the ATG translation initiation codon in mouse *Col2a1* NCBI reference sequence NM_031163.3. Genotyping of the identified mutant allele *Col2a1^{Rgsc856}* was performed by sequencing the PCR products amplified with the following primer pair: 5′-AAGTTCTAGCAAGCCACCCA-3′ and 5′-AGGACGGTTGGGTATCATCA-3′.

## Skeletal analysis

Embryos were eviscerated and fixed in 99% EtOH for 4 days. Alcian blue staining was performed in a solution of 80% EtOH, 20% acetic acid, and 0.015% Alcian blue for 4 days at 37°C. Specimens were rinsed and soaked in 95% EtOH for 3 days. Alizarin red staining was then performed in a solution of 0.002% alizarin red and 1% KOH for 12 h at room temperature. After rinsing with water, specimens were kept in 1% KOH solution until the skeletons became clearly visible. For storage, specimens were transferred into 50, 80, and finally 100% glycerol.

## Histological and immunohistochemical analysis

For histological analysis of mouse embryos, limbs were fixed in 4% paraformaldehyde (PFA) and decalcified in 10% EDTA for a week at 4°C. Hematoxylin & eosin (HE) and toluidine blue staining were performed using 6-μm paraffin sections according to standard protocols. For immunohistochemistry, paraffin sections were incubated with rabbit anti-type II collagen (Acris Antibodies, Hiddenhausen, Germany) or mouse anti-KDEL (MBL, Nagoya, Japan) antibodies. Primary antibodies were visualized with Alexa-conjugated goat anti-rabbit IgG (Molecular Probes®, Invitrogen, Carlsbad, CA, USA) and fluorescein-conjugated goat anti-mouse IgG antibodies (ICN Pharmaceuticals, Aliso Viejo, CA, USA). Stained cells were viewed using a fluorescence microscope or a confocal microscope (FV1000D; Olympus, Tokyo, Japan). To examine whether *Col2a1^{Rgsc856}* heterozygotes develop early-onset OA, knee and elbow joint samples from mice at 10 months of age were dissected, fixed in 4% PFA for 24 h, and defatted in alcohol. Then the samples were decalcified in 0.3 M EDTA (pH 7.5) for 10 days. Safranin O staining was performed using 4.5-μm paraffin sections. The severity of the OA lesion was evaluated using the modified Mankin scoring system, as described previously (Mankin et al. 1971; van der Sluijs et al. 1992).

## Electron microscope analysis

Limbs were fixed in 0.1 M sodium cacodylate buffer with 2.5% glutaraldehyde, decalcified in a 10% EDTA–Na_2 solution, and postfixed in 2% osmium tetroxide. After dehydration, they were embedded in EPON812. Semithin sections were stained with 1% toluidine blue to allow the selection of suitable areas for transmission electron microscopy. Ultrathin sections were stained with uranyl acetate and lead citrate. Visualization was performed using a Hitachi 7100 electron microscope (Hitachi, Tokyo, Japan) operated at 80 kV.

## RT-PCR analysis

Total RNA was extracted from rib cartilages at embryonic day (E) 18.5 using ISOGEN (Nippongene, Tokyo, Japan). Equal amounts of total RNA were reverse-transcribed into cDNA using TaqMan Multiscribe Reverse Transcriptase (Applied Biosystems). Each reverse transcription reaction (1 μl) was used as a template for SYBR® Green real-time PCR (Qiagen, Valencia, CA, USA). The following primers were used for amplification: 5′-TGAAGCTGCAGTA GAGGAGG-3′ and 5′-GGATATAAGCCATGGGGTC A-3′ for *Grp94*; 5′-GAGTCCCTGCCTTTCACCTT-3′ and 5′-CTGTCAGCCAAGCTAGGGAC-3′ for *Chop*; and 5′-A ACTGGGACGACATGGAGAA-3′ and 5′-GGGGTGTTG AAGGTCTAAA-3′ for *Actb*. SYBR Green PCR and real-time fluorescence detection were performed using an ABI PRISM 7700 Sequence Detection System (Applied Biosystems).

## Results

### Identification of a novel *Col2a1* mutation located in the C-propeptide coding region

ENU is a highly potent chemical mutagen that randomly induces multiple single-base-pair changes in genomic DNA at a very high efficiency (approximately $1 \times 10^{-3}$ per locus per gamete) (Hitotsumachi et al. 1985; Nolan et al. 1997). We screened 10,236 G1 mice (generated from crosses of ENU-mutagenized males and wild-type female mice) for abnormal skeletal phenotypes, especially focusing on the limb length transmitted as a dominant trait. We found one mutant line, termed M100856, that exhibits a

🖄 Springer
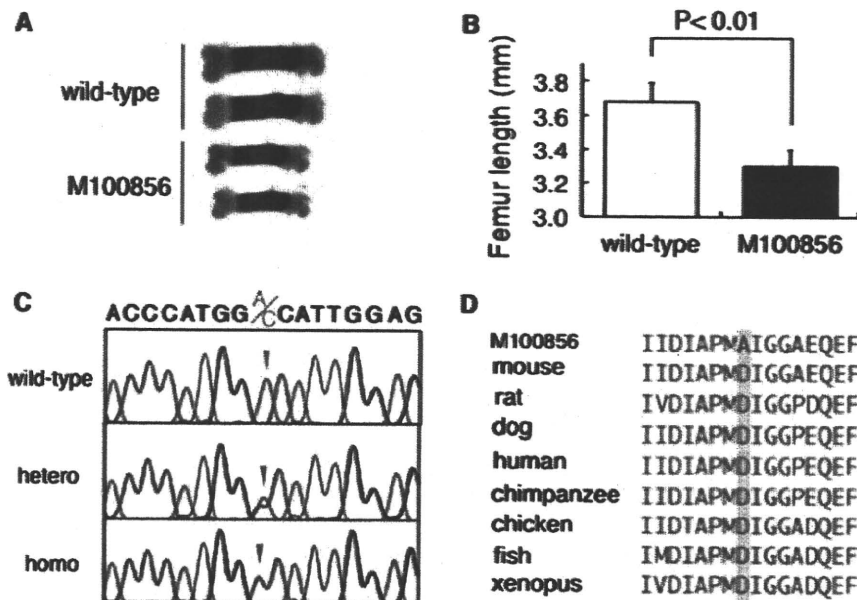
**Fig. 1** Identification of a novel missense mutation in *Col2a1* in mice mutagenized with ENU. **a** Gross appearance of femurs from wild-type and M100856 mice at E18.5. **b** Length of femurs from wild-type and M100856 mice at E18.5. Data are expressed as the mean ± SD ($n = 5$). The *p* value was determined using Student's *t*-test. The same result was obtained from the independent experiment conducted using E19.5 embryos. **c** cDNA sequence chromatograms from wild-type mice, *M100856* heterozygotes, and *M100856* homozygotes. The location of the mutation is indicated by the *orange arrowhead*. **d** Comparison of the amino acid sequences around the D1469 residue in various species. Amino acid residues identical to mouse type II collagen are represented by *blue* letters and those not identical by *red* letters. The location of D1469 is indicated by *orange* shading. D1469 is highly conserved

short-limb phenotype (posted at http://www.brc.riken.go.jp/lab/gsc/mouse/) (Fig. 1a, b).

Linkage analysis using the 103 backcross progeny showed that the *M100856* locus was localized to a 2.9-cM region on chromosome 15 (Electronic Supplementary Fig. 1). We checked the functions of all genes located in the linkage region and found two genes that have important functions in skeletogenesis, i.e., *Col2a1* and *Vdr*. Because previously reported heterozygous *Col2a1* mutant mice exhibited very mild skeletal phenotypes similar to M100856 mouse (Brown et al. 1981; Donahue et al. 2003; Li et al. 1995), we chose *Col2a1* as the most likely candidate gene. Sequencing of *Col2a1* cDNA derived from M100856 mutant mouse identified a missense mutation— c.4406A>C—which is predicted to cause an Asp-to-Ala substitution at position 1469 (p.D1469A) (Fig. 1c). The mutation was located in the coding region of the C-pro-peptide. This Asp residue was strongly conserved throughout various species (Fig. 1d). Interestingly, the Asp residue corresponding to mouse D1469 was substituted in the human *COL2A1* mutation responsible for PLSD-T, i.e., p.D1469H (Zankl et al. 2005). The mutation was also confirmed by sequencing of genomic DNA and was not found in ten inbred mouse strains. No other alterations in the *Col2a1* coding region were found. We designated this novel *Col2a1* mutant allele found in the M100856 line as

*Col2a1*$^{Rgsc856}$. The sequence chromatograms of the cDNA from *Col2a1*$^{Rgsc856}$ heterozygotes showed no difference in expression levels between wild-type and mutant alleles (Fig. 1c). We sequenced all the coding exons and the flanking regions of the other candidate gene, *Vdr*, which encodes vitamin D receptor, in M100856 mutants but we did not find any mutations.

### Skeletal and histological features of *Col2a1*$^{Rgsc856}$ mutants

*Col2a1*$^{Rgsc856}$ heterozygotes were mildly but significantly smaller than wild-type mice at E18.5 (Figs. 1a, b and 2). The limbs were disproportionately short (Fig. 2c), and the vertebral bodies were slightly hypoplastic (Fig. 2d). We generated *Col2a1*$^{Rgsc856}$ homozygotes by crossing the heterozygotes. The homozygotes died at birth, exhibiting severe dwarfism with shortened limbs and a shortened snout (Fig. 2a, b). The skeletal specimens also showed a severe skeletal dysplasia, including extremely shortened limbs (Fig. 2c), severe spondylar dysplasia (Fig. 2d), severe pelvic hypoplasia (Fig. 2e), and brachydactyly (Fig. 2f). These defective skeletal features of the homozygotes are similar to those observed in PLSD-T patients.

To understand the pathogenic basis for the skeletal dysplasia phenotype, we investigated the histology of the